

Measurement of Whistler Wave Dispersion Relation

Nathan Solomon, Juri Alhuthali
University of California, Los Angeles
 (Dated: April 16, 2025)

We used a dipole antenna inside a cylindrical plasma chamber to launch electromagnetic waves with a known temporal frequency, between 40 and 120 MHz. By placing a small \vec{B} -probe made of 3 orthogonal wire loops inside the chamber and recording the electromotive force around each loop, we were able to take advantage of Faraday’s law to calculate the magnetic flux at various positions and times in the plasma. After further manipulating the wave equation, I used the data from the \vec{B} -probe to derive an experimental dispersion relation for the whistler waves. Fitting the theoretical dispersion relation to the experimental one allowed me to calculate a confidence interval for the density of the plasma, which contradicts the results from Solomon et al.[1]

I. INTRODUCTION

A whistler wave is a type of electromagnetic wave that occurs in a plasma. It is called “whistler” because when it occurs in the Earth’s ionosphere, it is in the audible range of frequencies, and to an observer, the frequency appears to decrease exponentially over time. The reason for that is that higher frequency components of a wave travel faster in the same medium, so they reach an observer before the lower frequency components do.

There are many types of waves which can propagate through a plasma. The derivation of the equation for whistler waves is beyond scope of this paper, but we can still identify whistler waves because we know that they are right-hand circularly polarized, and they propagate in the same direction as the magnetic field.[2]

The dispersion relation for a whistler wave is given by equation 1, where $k_{||}$ is the component of the wave vector which is parallel to the magnetic field, $\omega_{ce} = eB_z/m_e$ is the electron gyrofrequency, $\delta_e := c/\omega_{pe}$ is the electron inertial wavelength, $\omega_{pe} = e\sqrt{n/(\epsilon_0 m_e)}$ is the electron plasma frequency, and n is the number density. Since we configured B_z to be $70G = 0.007T$, the dispersion relation depends only on the density n , meaning that once we obtain an experimental dispersion relation, we can use it to measure n .

$$2\pi f = \omega = \omega_{ce} \frac{k_{||}^2 \delta_e^2}{1 + k_{||}^2 \delta_e^2} \quad (1)$$

To create the whistler waves, we first create a uniform plasma in a cylindrical chamber. The “180E machine” which has been designed for this class[3] contains argon gas at 1 mTorr of pressure and has been configured to create a uniform axial 70 Gauss magnetic field.[4] The 180E machine (FIG. 1) uses a radio frequency voltage discharge with a peak-to-peak amplitude of 300 Volts to create a plasma via field ionization. During the discharge, there is a lot of high-frequency electromagnetic noise present which makes analyzing the plasma extremely difficult[1], so we perform all experiments during the afterglow – that is, the period of a few milliseconds after the discharge during which the plasma gradually dissipates. For this particular experiment, we wait until 1 millisecond into

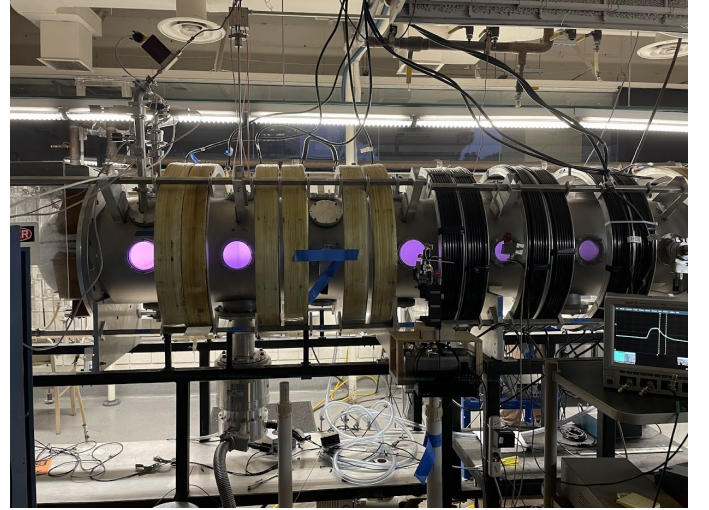


FIG. 1. Photo of the “180 machine”, which is a vacuum chamber with a plasma inside. The purple windows are the ports, and the yellow and black rings are the confining magnets.

the afterglow, at which point we use a dipole antenna at port 3 of the 180E machine to launch a whistler wave.

To measure the wave amplitude, we used a \vec{B} -probe, which is made of 3 perpendicular loops of wire, each in the shape of a circle with radius 1.3 centimeters. Faraday’s law of induction states that a changing magnetic flux through one of the loops will create a curling electric field, which causes current to flow through that loop of wire:

$$\epsilon = -\frac{d\Phi}{dt}. \quad (2)$$

We can then measure this EMF (ϵ) and integrate it over time to obtain the magnetic field (up to a constant).

II. EXPERIMENTAL SETUP

In order to launch the wave, we configure a waveform generator to generate a pulse with a duration of 5 wavelengths at the desired frequency $f \in [40MHz, 120MHz]$.

Before going to the antenna, the waveform generator sends the signal to a 10x amplifier so that the peak-to-peak voltage becomes 17V, as well as a low-pass filter to cut off unwanted harmonics. When applying pulses at 50-120 MHz, we used a 98 MHz low-pass filter, and when applying pulses at 40 MHz, we used a 60 MHz low-pass filter. After the filter, the signal was sent to the antenna, where the 5 pulses triggered the formation of a whistler wave with the same frequency, which then propagated along the z axis (that is, along the axis of the cylindrical chamber). We chose to use a duration of 5 wavelengths, because looking at a longer window of time allows us to calculate the spatial frequency more precisely, but if we had continued the antenna pulse for longer, the whistler waves would begin colliding with their own reflections.

To measure the whistler waves propagating through the plasma, we placed a \vec{B} -probe inside the 180E machine along the z -axis and recorded the electromotive force on each of the loops of wire from 1 ms after the discharge to 1.0005 ms after the discharge. We repeated that 5 times for each position and averaged the results in order to reduce the amount of noise. Since most of the energy which the dipole antenna puts into the plasma is either lost to Landau damping, or travels in some direction which does not make it reach the small \vec{B} probe, we had to amplify the signals measured by the \vec{B} probe by a factor of 10,000 in order to be able to record them. After amplifying the signals, we recorded the measured electromotive forces on each loop of wire in an HDF5 file so that we could analyze the data conveniently using Python.

III. RESULTS AND ANALYSIS

The HDF5 files from our data analysis describe the EMF felt by each of the 3 loops of the \vec{B} -probe as a function of time t after launching the wave, the z coordinate (where the dipole antenna is at $z = 0$), and the frequency f applied by the antenna.

Integrating $\vec{B}(z, t, f)$ over time and then dividing by the loop area πr^2 (where $r = 1.3\text{cm}$) gives the magnetic field $B(z, t, f)$. However, integrating causes noise in the signal to accumulate over time, creating the horizontal streaks in FIG. 2 which resemble “VGA ghosting” (a type of artifact appearing in monitors with damaged or loose analog cables). Because of that, I chose to do the remainder of the data analysis using the time derivative $\dot{\vec{B}}(z, t, f)$ instead of $B(z, t, f)$ itself. This is a valid decision, because B and \dot{B} have the same wave vector k , the same temporal frequency f , and the same damping coefficient λ .

In order to extract the wave vector k from our data, it is helpful to define a new quantity $\vec{\dot{B}} = \dot{B}_x + i\dot{B}_y$. Since we only care about the component of the wave that is right-hand circularly polarized and propagating in the $-z$ direction, this new quantity describes all the behavior of the whistler wave that we are interested in analyzing. Now, $\vec{\dot{B}}$ is a complex-valued function, so we can visualize

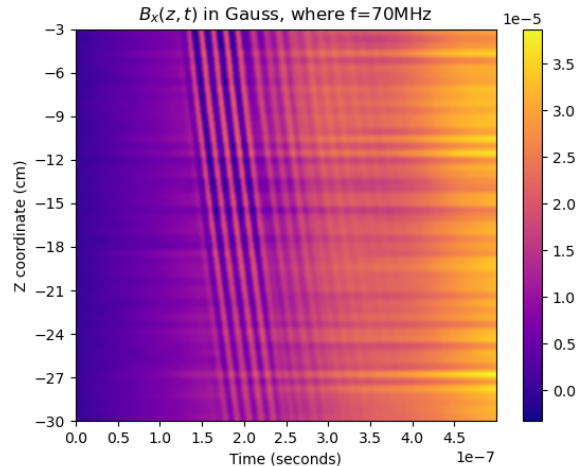


FIG. 2. Plot of $B_x(z, t, f = 70\text{MHz})$

its behavior (for each f) by plotting it in Hue-Saturation-Value color space, as is common for complex-valued functions. For the point at (t, z) on the plot, the hue (H) is equal to the phase of $\vec{\dot{B}}(t, z)$, the value (V) is proportional to the amplitude, and the saturation (S) is always 100%. An example of such a plot is shown in FIG. 3 for the case where $f = 70\text{MHz}$.

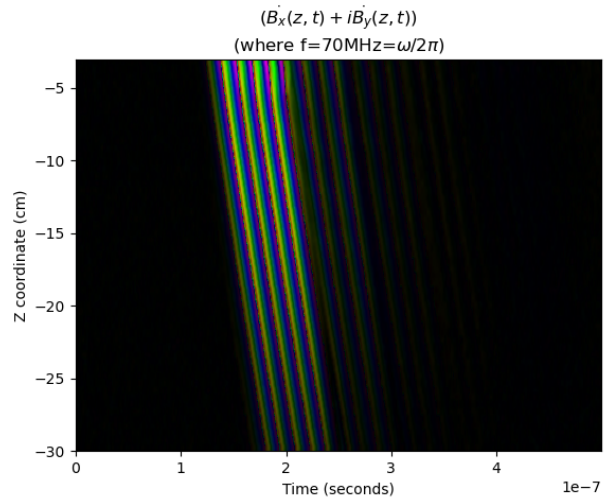


FIG. 3. Representation of a complex valued function in HSV color space, where hue corresponds to phase, saturation is always 100%, and value corresponds to magnitude.

Since we see the hues loop around a full rainbow more than 5 times as we go from the left side of FIG. 3 to the right side, we can infer that more than 5 pulses are passing through each point. In fact, the fainter bands in FIG. 3 come from the wave not just propagating in the $-z$ direction, but also moving in the $+z$ direction and reflecting off the edge of the chamber, so they propagate in the $-z$ direction at a later time (having already been

partially damped, which is why they are fainter). Since the waves that have been reflected and the waves that haven't been reflected could have different phases at the same z position, I manually cropped off what appears to be the fainter portions of the graph, in order to simplify the remainder of the data analysis process.

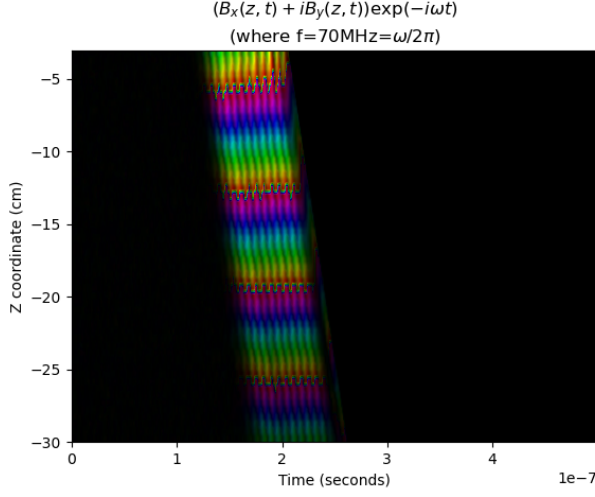


FIG. 4. Multiplying the data from the previous figure by $\exp(-i\omega t)$ cancels out a majority of the time dependence.

If we temporarily assume that our complex-valued function $\dot{B}(z, t, f)$ perfectly follows the solution to the wave equation for a wave propagating in the $-z$ direction, we have $\dot{B}(z, t, f) = \exp(i(\omega t + kx))$. This is not actually true because it does not account for damping, or for regions where the wave has already passed or has not yet passed, but it is useful for mathematically justifying the following step: we can cancel out the time-dependence by multiplying by $\exp(-i\omega t)$. After doing that and cropping out the reflected waves as described above, we obtain the complex-valued function shown in FIG. 4. Since this no longer depends on time, we can average over t to obtain a new complex-valued function, $\dot{B}(z, f)$, which is shown in FIG. 5.

Since the phase and magnitude of $\dot{B}(z, t) \exp(-i\omega t)$ does not depend on time, we can average over all times to obtain $\dot{B}(z)$, and by averaging so many signals, we dramatically reduce the amount of noise. At this point, $\dot{B}(z)$ should very closely resemble a sinusoid whose magnitude decays exponentially as a function of distance from the source (which is at the positive z end of the chamber).

For each f , by fitting the magnitude of $\dot{B}(z, f)$ to an exponential of the form $A \exp(rz)$ and fitting the real component of $\dot{B}(z)$ to a sinusoid of the form $A \cos(kx + \phi)$ using SciPy's "optimize.curve_fit" method, we obtain the wavenumber k and the damping coefficient $\lambda = 1/r$ for each f , as well as error margins for both k and λ . An example curve fit is shown in FIG. 5.

That data for k and λ as a function of f is shown in the following table, which also includes the Q -factor. The

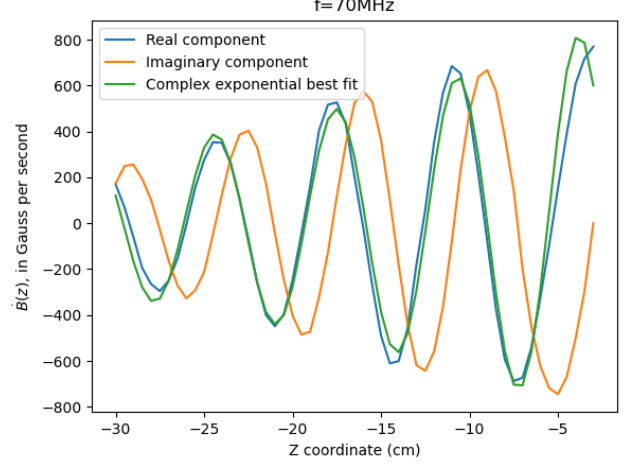


FIG. 5. An example of a curve fit used for calculating k and λ at 70 MHz.

Q -factor is defined as

$$Q := \sqrt{\frac{\lambda^2 + k^2}{2\lambda}}, \quad (3)$$

and it is used to describe how underdamped an oscillator is, with larger Q corresponding to more underdamped systems.

f (MHz)	k (cm^{-1})	λ (cm^{-1})	Q
40	0.6477 ± 0.0226	0.0688 ± 0.0020	4.74
50	0.7164 ± 0.0209	0.0617 ± 0.0027	5.83
60	0.8076 ± 0.0143	0.0464 ± 0.0028	8.72
70	0.9161 ± 0.0122	0.0363 ± 0.0029	12.63
80	1.0222 ± 0.0104	0.0254 ± 0.0036	20.11
90	1.1338 ± 0.0090	0.0193 ± 0.0042	29.41
100	1.2557 ± 0.0081	0.0172 ± 0.0044	36.51
110	1.3893 ± 0.0092	0.0204 ± 0.0048	34.04
120	1.5334 ± 0.0127	0.0311 ± 0.0063	24.66

Now that we have found k as a function of f , we can plot the experimental dispersion relation and fit it to the theoretical dispersion relation given in equation 1. Note that I am assuming the density is roughly uniform throughout the region which the waves propagate through, since it would be extremely difficult to redo these calculation for a plasma with non-uniform density.

The result is shown in FIG. 6. The theoretical fit lies entirely within the error bounds of the experimental fit, which indicates that the whistler waves are following the physics we expect them to. However, the calculated density n differs dramatically from the 95% confidence interval calculated in Solomon et al.[1]

The curve fit shown in FIG. 6 gives the following 95% confidence interval on the density of the plasma:

$$n = (4.2866 \pm .0643) \times 10^{17} \text{ m}^{-3}. \quad (4)$$

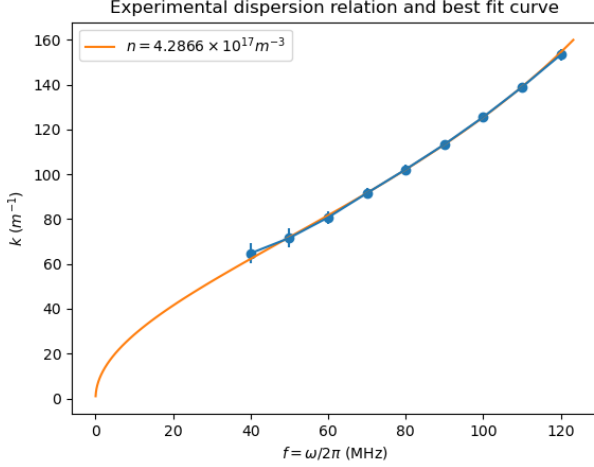


FIG. 6. A theoretical dispersion relation for a whistler wave (shown in orange) has been fitted to the dispersion relation which I experimentally derived (shown with 95% error bars, in blue)

IV. DISCUSSION

This new calculated value for the plasma density challenges the claim by Solomon et al.[1] that the number density on the axis of the 180E machine is, with 95% confidence, between 0.9×10^{17} and 1.7×10^{17} particles per cubic meter (1 ms into the afterglow, when the pressure is 1 mTorr, the electromagnets are creating a uniform 70G field, and the RF discharge peak-to-peak amplitude is 300V). Given the unreliability of using automated analysis of Langmuir probes[1], we can safely assume that the density is closer to $4.29 \times 10^{17} m^{-3}$. Additionally, the smaller confidence interval on n using this method indicates that this method is more precise, although not necessarily more accurate. However, this new calculation of n could still be unreliable, since calculating the density using the dispersion relation required assuming the density is constant throughout the 180E machine, which we know is not true.

If we suppose that the actual density of the plasma is indeed $(4.2866 \pm .0643) \times 10^{17} m^{-3}$, then by obtaining experimental data whose confidence intervals contain the theoretical fit, we have verified the theoretical dispersion relation for whistler waves. Also, by noticing that in FIG. 5, the imaginary component of $\vec{B}(z, f)$ (that is, $\vec{B}_y(z, f)$) lags the real component (that is, $\vec{B}_x(z, f)$) by $\pi/2$ radians, we can confirm that the electromagnetic waves we are observing are right-hand circularly polarized.

Lastly, we want to verify that the whistler waves are propagating primarily along the z -axis, parallel to the magnetic field. To do so, we moved the \vec{B} -probe not only in the z direction, but also in the x direction, and for each (x, y) position, we calculated the root-mean-

square (RMS) voltage measured by the \vec{B} -probe to obtain a rough approximation of the energy of the whistler wave traveling through each point in the xz -plane. Once again, this was averaged over 5 shots for each position. The results at both $f = 40 MHz$ and $f = 120 MHz$ are shown in FIG. 7.

Those plots indicate that at higher frequencies, the whistler waves move in a straighter path. However, the cloud seen at $\theta \approx -10^\circ$ in the $f = 40 MHz$ plot may be due to some other error, since it appears to be part of a separate “blob” from the rest of the whistler wave.

For future experiments, it would be interesting to look at more of these xz -planes to characterize how the spread and lopsidedness of the wave’s trajectory depends on frequency.

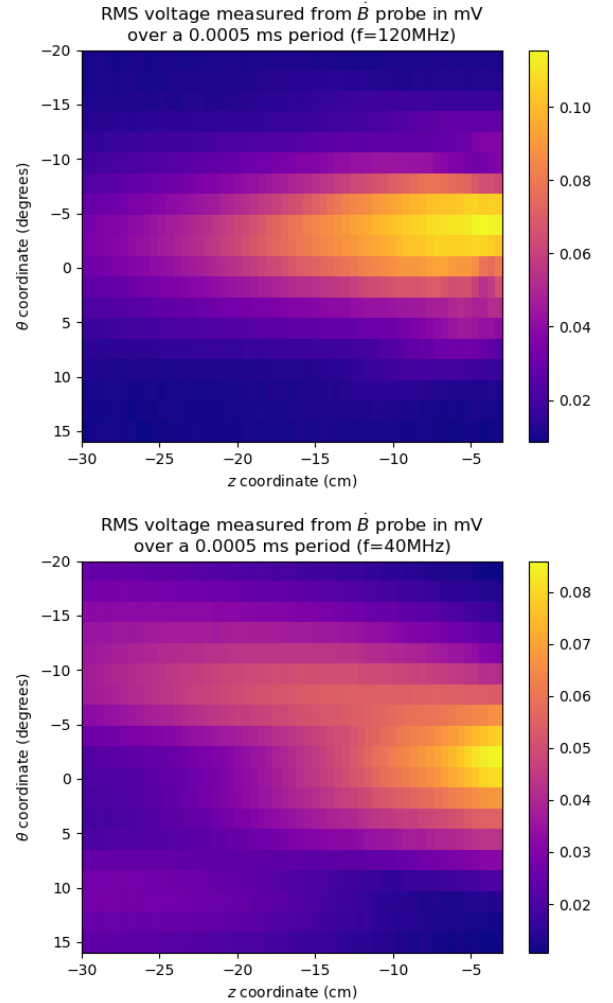


FIG. 7. Visualization of the direction in which the wave travels. The \vec{B} probe rotates about an axis along the bottom of the chamber (parallel to the z axis), so if we use a small-angle approximation, θ is a proxy for the x coordinate, and we’re actually looking at an xz -plane.

-
- [1] N. Solomon and J. Alhuthali, Characterization of a plasma using langmuir probing (2025).
 - [2] D. Schaeffer, Winter 2025 lecture slides for physics 180e: plasma laboratory (2025).
 - [3] W. Gekelman, P. Pribyl, Z. Lucky, S. W. Tang, J. Han, and Y. Qian, Design, construction and utilization of a university plasma laboratory, *Journal of Plasma Physics* **86**, 925860301 (2020).
 - [4] J. Perez, Icpd_magnetifieldsolver_w25.py, python script to calculate magnetic field in the 180E machine as a function of current through each magnet.